Data-driven Based Coordinated Voltage Control for Active Distribution Networks with Multiple Devices

Shunqi Zeng[1], Fei Wang[1], Xin Li[1], Ziqi Zhang[2*], Yue Zhou[3], Hao Yu[2], Haoran Ji[2]

[1] Guangzhou Power Supply Bureau, Guangdong Power Grid Co., Ltd., Guangzhou 510620, China
[2] Key Laboratory of Smart grid of Ministry of Education, Tianjin University, Tianjin 300072, China
[3] Institute of Energy, School of Engineering, Cardiff University, Cardiff CF24 3AA, UK
ziqizhang_97@tju.edu.cn

Abstract. The integration of distributed generation (DG) has increased significantly. This has resulted in more voltage violations in the active distribution network (ADN). Coordination of various control devices is an effective way to address voltage problems. Given the lack of accurate network parameters in practical operation, a data-driven approach can be employed to facilitate voltage control in ADN. In this paper, a data-driven voltage control strategy for ADN is proposed to suppress voltage fluctuations. First, the network parameters of ADN are identified using a data-driven method. Then, a coordinated voltage control model is established to enable multiple regulation devices to work together. Finally, the effectiveness of the proposed control strategy is validated through the modified IEEE 33-node distribution system. The data-driven voltage control method proposed here can significantly improve the voltage profile of ADN.

Keywords: Active distribution network (ADN), distributed generator (DG), data-driven control.

1 Introduction

The extensive integration of distributed generators (DGs) [1] has a significant impact on the flexible operation [2] of active distribution networks (ADNs). The high penetration of DGs causes notable uncertainties in temporal distribution [3], which can result in a sharp fluctuation of feeder power and considerable voltage violations [4].

Multiple regulation devices, including discrete and continuous regulation devices, have been implemented to enhance the voltage performance of ADNs [5]. The discrete regulation devices, such as on load tap changers (OLTC) and capacitor banks (CB), can modify the operation of ADNs over extended periods of time [6]. However, discrete regulation devices have slow response times and limited action frequency [7], making it difficult to suppress frequent voltage fluctuations [8]. Therefore, these devices are typically regulated day-ahead based on prediction information [9]. The smart inverter of DG is a novel continuous regulation device that provides reactive power for fast voltage control [10]. The coordination of multiple devices is a critical issue that needs to be addressed.

Model-based control methods are commonly utilized for determining the strategies of multiple devices. Ref. [11] proposed a two-stage algorithm to coordinate the available reactive power of DG and OLTC with multiple optimization objectives. A hierarchical approach was suggested in [12], which could regulate voltages in a weak subtransmission network by coordinating OLTC, CBs, and load aggregators. Additionally, Ref. [13] proposed a distributed coordinated voltage control scheme for distribution networks with DGs and OLTC. Coordinated voltage control was achieved for multiple devices according to a three-stage incentive-based framework in [14]. However, accuracy and complexity challenges may limit the efficacy of the model-based control method, which is reliant upon precise network parameters for ADNs.

Preliminary studies of data-driven optimization have been conducted in ADNs. As a typical data-driven method, machine learning has been studied extensively. To combat the uncertainties surrounding renewable energy, Ref. [15] proposed a data-driven multistage adaptive robust optimization framework utilizing a reinforcement learning methodology. Additionally, a deep reinforcement learning-based method was proposed in [16] for voltage regulation in distribution networks with extensive photovoltaic (PV) penetration. A deep reinforcement learning approach was proposed in [17] to control nodal voltage without full ADN topology and parameters. Model-free adaptive control (MFAC) is another conventional data-driven approach that builds a control model using the input-output data of the controlled system [18]. Ref. [19] introduced the concept of prediction control in MFAC to improve control performance with time-series characteristics. However, these methods may require a lengthy iteration or training process, resulting in a significant time overhead.

In this paper, a data-driven based voltage control strategy of ADN is proposed. The main contributions are summarized as follows.

1) A data-driven based parameter estimation method is realized with the historical data of ADN. The relationship between nodal voltages and injected currents is firstly expressed by the power flow analysis for ADNs. Through mining the potential relationship from historical data, the network parameters of ADN can be obtained to support the establishment of optimization model.

2) An optimization model considers the cooperation of multiple regulation devices is established to eliminate voltage violations. With the forecast of loads and DGs, the coordinated control strategy of multiple regulation devices can be determined effectively while minimizing the operation costs of ADN.

The paper is organized as follows. Section II explains a method of data-driven parameter estimation. Section III determines the control strategy for multiple controllable devices. Section IV presents case studies on the modified IEEE 33-node distribution system. Finally, Section V summarizes the conclusions.

2 Data-driven Based Physical Parameter Estimation for ADN

Based on the power flow analysis for ADNs, the relationship between nodal voltages and injected currents can be expressed as Eq. (1).

$$\boldsymbol{U} = \boldsymbol{Z}\boldsymbol{I} \tag{1.a}$$

$$\begin{bmatrix} \widetilde{U}_{1,t} \\ \widetilde{U}_{2,t} \\ \vdots \\ \widetilde{U}_{i,t} \\ \vdots \\ \widetilde{U}_{N,t} \end{bmatrix} = \begin{bmatrix} \tilde{Z}_{1,1} & \tilde{Z}_{1,2} & \cdots & \tilde{Z}_{1,j} & \cdots & \tilde{Z}_{1,N} \\ \tilde{Z}_{2,1} & \tilde{Z}_{2,2} & \cdots & \tilde{Z}_{2,j} & \cdots & \tilde{Z}_{2,N} \\ \vdots & \vdots & \vdots & \vdots & \vdots & \vdots \\ \tilde{Z}_{i,1} & \tilde{Z}_{i,2} & \cdots & \tilde{Z}_{i,j} & \cdots & \tilde{Z}_{i,N} \\ \vdots & \vdots & \vdots & \vdots & \vdots & \vdots \\ \tilde{Z}_{N,1} & \tilde{Z}_{N,2} & \cdots & \tilde{Z}_{N,j} & \cdots & \tilde{Z}_{N,N} \end{bmatrix} \begin{bmatrix} \tilde{I}_{1,t} \\ \tilde{I}_{2,t} \\ \vdots \\ \tilde{I}_{i,t} \\ \vdots \\ \tilde{I}_{N,t} \end{bmatrix} \tag{1.b}$$

where $\tilde{Z}_{i,j}$ is the element of the bus impedance matrix at the ith row jth column, which can be calculated as $\tilde{Z}_{i,j} = R_{i,j} + \mathrm{j}X_{i,j}$.

In [20], a node impedance matrix estimation method is proposed based on the nodal measurements. Without the prior information of ADN, $\tilde{Z}_{i,j}$ is expressed as follows:

$$R_{i,i} = -\frac{V_i^2\left(-P_i\left(g_{i,i}^{\mathrm{P}}\right)^2 - 2Q_i g_{i,i}^{\mathrm{P}} g_{i,i}^{\mathrm{Q}} + V_i g_{i,i}^{\mathrm{P}} + P_i\left(g_{i,i}^{\mathrm{Q}}\right)^2\right)}{\left(P_i^2+Q_i^2\right)\left(\left(g_{i,i}^{\mathrm{P}}\right)^2+\left(g_{i,i}^{\mathrm{Q}}\right)^2\right) - 2V_i\left(P_i g_{i,i}^{\mathrm{P}} + Q_i g_{i,i}^{\mathrm{Q}}\right) + V_i^2} \tag{2.a}$$

$$X_{i,i} = -\frac{V_i^2\left(Q_i\left(g_{i,i}^{\mathrm{P}}\right)^2 - 2P_i g_{i,i}^{\mathrm{P}} g_{i,i}^{\mathrm{Q}} + V_i g_{i,i}^{\mathrm{Q}} - Q_i\left(g_{i,i}^{\mathrm{Q}}\right)^2\right)}{\left(P_i^2+Q_i^2\right)\left(\left(g_{i,i}^{\mathrm{P}}\right)^2+\left(g_{i,i}^{\mathrm{Q}}\right)^2\right) - 2V_i\left(P_i g_{i,i}^{\mathrm{P}} + Q_i g_{i,i}^{\mathrm{Q}}\right) + V_i^2} \tag{2.b}$$

$$R_{i,j} = \frac{A\cdot(B_{\mathrm{R}}+C_{\mathrm{R}})}{D}, X_{i,j} = \frac{-A\cdot(B_{\mathrm{X}}+C_{\mathrm{X}})}{D}, \forall i,j \in \Omega_{\mathrm{n}} \tag{2.c}$$

$$A = V_j\left(P_i^2 R_{i,i}^2 + P_i^2 X_{i,i}^2 + Q_i^2 R_{i,i}^2 + Q_i^2 X_{i,i}^2 - V_i^4\right) \tag{2.d}$$

$$D = V_i^2\begin{pmatrix} P_i^2 R_{i,i}^2 + P_i^2 X_{i,i}^2 + 2P_i R_{i,i} V_i^2 + \\ Q_i^2 R_{i,i}^2 + Q_i^2 X_{i,i}^2 + 2Q_i X_{i,i} V_i^2 + V_i^4 \end{pmatrix} \tag{2.e}$$

$$B_{\mathrm{R}} = \left(g_{i,j}^{\mathrm{P}}\cos\left(\theta_i-\theta_j\right) - g_{i,j}^{\mathrm{Q}}\sin\left(\theta_i-\theta_j\right)\right)\left(V_i^2 + P_i R_{i,i} + Q_i X_{i,i}\right) \tag{2.f}$$

$$C_{\mathrm{R}} = \left(g_{i,j}^{\mathrm{P}}\sin\left(\theta_i-\theta_j\right) + g_{i,j}^{\mathrm{Q}}\cos\left(\theta_i-\theta_j\right)\right)\left(-P_i X_{i,i} + Q_i R_{i,i}\right) \tag{2.g}$$

$$B_{\mathrm{X}} = -\left(g_{i,j}^{\mathrm{P}}\sin\left(\theta_i-\theta_j\right) + g_{i,j}^{\mathrm{Q}}\cos\left(\theta_i-\theta_j\right)\right)\left(V_i^2 + P_i R_{i,i} + Q_i X_{i,i}\right) \tag{2.h}$$

$$C_{\mathrm{X}} = \left(g_{i,j}^{\mathrm{P}}\cos\left(\theta_i-\theta_j\right) - g_{i,j}^{\mathrm{Q}}\sin\left(\theta_i-\theta_j\right)\right)\left(-P_i X_{i,i} + Q_i R_{i,i}\right) \tag{2.i}$$

where $g_{i,j}^{\mathrm{P}}$ and $g_{i,j}^{\mathrm{Q}}$ represent the active and reactive sensitivity functions of the voltage variables at node i to the nodal power injection at node j, respectively.

Further inverting the nodal impedance matrix $\boldsymbol{Z}$, the node admittance matrix $\boldsymbol{Y}$ of distribution network can be obtained as follows.

$$\boldsymbol{Y}=\boldsymbol{Z}^{-1}=\begin{bmatrix}\tilde{Y}_{1,1} & Y_{1,2} & \cdots & \tilde{Y}_{1,j} & \cdots & \tilde{Y}_{1,N}\\ \tilde{Y}_{2,1} & \tilde{Y}_{2,2} & \cdots & \tilde{Y}_{2,j} & \cdots & \tilde{Y}_{2,N}\\ \vdots & \vdots & \vdots & \vdots & \vdots & \vdots\\ \tilde{Y}_{i,1} & \tilde{Y}_{i,2} & \cdots & \tilde{Y}_{i,j} & \cdots & \tilde{Y}_{i,N}\\ \vdots & \vdots & \vdots & \vdots & \vdots & \vdots\\ \tilde{Y}_{N,1} & \tilde{Y}_{N,2} & \cdots & \tilde{Y}_{N,j} & \cdots & \tilde{Y}_{N,N}\end{bmatrix} \tag{3}$$

where $\tilde{Y}_{i,j}$ is the element of the bus admittance matrix at the ith row jth column, which is calculated by the resistance and reactance of the line as $\tilde{Y}_{i,j}=1/\left(\hat{r}_{ij}+\mathrm{j}\hat{x}_{ij}\right)$.

Thus, the network parameters of ADN are expressed by the voltage sensitivity and nodal injected power.

However, the voltage sensitivity function of ADN is a multivariate complex nonlinear relation, which is not easy to be obtained in practical operation. The high-dimensional voltage sensitivity is described as Eq. (4).

$$\Delta V_i=g_{i,j}^{\mathrm{P}}\left(\Delta\rho_j\right)\big|_{V=V_0}+g_{i,j}^{\mathrm{Q}}\left(\Delta\rho_j\right)\big|_{V=V_0} \tag{4}$$

The rapid development of artificial intelligence offers a promising approach for extracting voltage sensitivity functions. This study employs a neural network method to extract the voltage sensitivity function of ADN using heterogeneous historical data. By hierarchically transforming the raw input from layer to layer, the neural network can learn high-dimensional abstract feature representations from the historical operational data. Then, the neural network-fitted voltage sensitivity function is utilized to facilitate identification of the network parameters.

3 Coordinated Voltage Control Strategy with Estimated Physical Parameter

Based on the estimated network parameters, a coordinated voltage control model is established with the forecast information.

Objective function. Accounting for the operational efficiency and voltage profile of ADNs, the objective is set to minimize the voltage deviation and total power loss, which is formulated as:

$$\min f=W_\alpha f_{\mathrm{L}}+W_\beta f_V \tag{5.a}$$

$$f_{\mathrm{L}}=\sum_{t=1}^{T}\sum_{ij\in\Omega_{\mathrm{b}}}\hat{r}_{ij}I_{t,ij}^2 \tag{5.b}$$

$$f_{\mathrm{V}}=\sum_{t=1}^{T}\sum_{i\in\Omega_{\mathrm{n}}}\left|V_{t,i}^2-1\right|,V_{t,i}\geq V_{\mathrm{thr}}^{\max}||V_{t,i}\leq V_{\mathrm{thr}}^{\min} \tag{5.c}$$

Operational constraints. The proposed coordinated voltage control model imposes constraints on ADN and discrete/continuous regulation devices. These constraints are described as follows.

ADN operation constraints. Based on the estimated network parameters of ADN, the DistFlow branch model serves as the operational constraints of ADN. This model can be described mathematically as follows.

$$\sum_{ji\in\Omega_\mathrm{b}}\left(P_{t,ji}-\hat{r}_{ij}I_{t,ji}^2\right)+P_{t,i}=\sum_{ik\in\Omega_\mathrm{b}}P_{t,ik} \tag{6.a}$$

$$\sum_{ji\in\Omega_\mathrm{b}}\left(Q_{t,ji}-\hat{x}_{ij}I_{t,ji}^2\right)+Q_{t,i}=\sum_{ik\in\Omega_\mathrm{b}}Q_{t,ik} \tag{6.b}$$

$$V_{t,i}^2-V_{t,j}^2+\left(\left(\hat{r}_{ij}\right)^2+\left(\hat{x}_{ij}\right)^2\right)I_{t,ij}^2=2\left(\hat{r}_{ij}P_{t,ij}+\hat{x}_{ij}Q_{t,ij}\right) \tag{6.c}$$

$$I_{t,ij}^2V_{t,i}^2=P_{t,ij}^2+Q_{t,ij}^2 \tag{6.d}$$

$$P_{t,i}=P_{t,i}^{\mathrm{DG}}-P_{t,i}^{\mathrm{LOAD}},Q_{t,i}=Q_{t,i}^{\mathrm{DG}}+Q_{t,i}^{\mathrm{CB}}-Q_{t,i}^{\mathrm{LOAD}} \tag{6.e}$$

$$(V^{\min})^2\le V_{t,i}^2\le(V^{\max})^2,I_{t,ij}^2\le\left(I_{ij}^{\max}\right)^2 \tag{6.f}$$

Discrete devices operation constraints. Discrete regulation devices may consist of various types of equipment, including on-load tap changers (OLTC), circuit breakers (CBs), and tie switches. These devices are limited in their ability to adjust the system's operating state due to the number of available actions. This paper provides examples of how OLTC and CBs can be used to demonstrate the coordinated voltage control model. The operation constraints of OLTC and CB are described as Eq. (7) and Eq. (8), respectively.

$$V_{t,i}=k_{t,ij}V_{t,j} \tag{7.a}$$

$$k_{t,ij}=k_{ij,0}+K_{t,ij}\Delta k_{ij} \tag{7.b}$$

$$\sum_{t=1}^{N_\mathrm{T}}\left|K_{t,ij}-K_{t-1,ij}\right|\le\Delta^{\mathrm{OLTC,max}} \tag{7.c}$$

$$-K_{ij}^{\max}\le K_{t,ij}\le K_{ij}^{\max},K_{t,ij}\in\mathbb{Z} \tag{7.d}$$

$$Q_{t,i}^{\mathrm{CB}}=N_{t,i}^{\mathrm{CB}}\cdot q_i^{\mathrm{CB}} \tag{8.a}$$

$$\sum_{t=1}^{N_\mathrm{T}}\left|N_{t,i}^{\mathrm{CB}}-N_{t-1,i}^{\mathrm{CB}}\right|\le\Delta^{\mathrm{CB,max}} \tag{8.b}$$

$$0\le N_{t,i}^{\mathrm{CB}}\le N^{\mathrm{CB,max}},\ N_{t,i}^{\mathrm{CB}}\in\mathbb{Z} \tag{8.c}$$

Continuous devices operation constraints. Continuous regulation devices mainly include DG inverters and static var compensator (SVC), which can respond to rapid power fluctuations in short time-scales. We take DG inverters as an example to represent continuous regulation devices in the voltage control of ADN.

$$\underline{Q}_i^{\mathrm{DG}} \le Q_{t,i}^{\mathrm{DG}} \le \bar{Q}_i^{\mathrm{DG}} \tag{9.a}$$

$$0 \le \sqrt{\left(P_{t,i}^{\mathrm{DG}}\right)^2 + \left(Q_{t,i}^{\mathrm{DG}}\right)^2} \le S_i^{\mathrm{DG}} \tag{9.b}$$

Based on the above analysis, the coordinated voltage control model can be expressed in the following form:

$$\min f = W_\alpha f_{\mathrm{L}} + W_\beta f_V \tag{10.a}$$

$$\mathrm{s.t.}\quad (5),(6),(7),(8),(9) \tag{10.b}$$

4 CASE STUDIES AND ANALYSIS

In this section, the effectiveness of the proposed data-driven based coordinative strategy of ADN is verified using the modified IEEE 33-node distribution system. The numerical experiments were conducted on a computer with an Intel(R) Core(TM) i7-9750H CPU processor running at 2.60 GHz and 16 GB of RAM.

4.1 Modified IEEE 33-node Distribution System

The modified IEEE 33-node distribution system includes a substation and 32 branches, of which the rated voltage level is 12.66 kV. The structure of the test system is shown in Fig. 1.

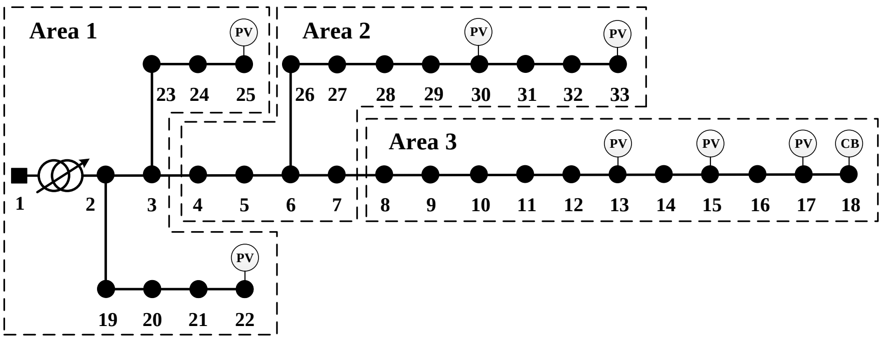

Fig. 1. Structure of the modified IEEE 33-node distribution system.

The total active power and reactive power demands are 3715.0 kW and 2300.0 kvar. We assume that the distribution system is divided into three areas. To consider the high DG penetration, 7 PV units with 400.0 kVA capacity each are integrated in the test system. There is an OLTC with ten tap steps and a regulation of 1% per tap between the node 1 and 2. Besides, the CBs of 60 kvar with five units are connected to node 18. Considering the action frequency limited of discrete regulation devices, $\Delta^{\mathrm{OLTC,max}}$ and $\Delta^{\mathrm{CB,max}}$ are all set as 4 times per day with a minimum action interval of 1h. The control period is set as 15min. The forecasting curves of DG generation and load operation are shown in Fig. 2. The upper and lower limits of the statutory voltage range of ADN are set as 1.10 p.u. and 0.90 p.u. The desired voltage range is set from 0.95 p.u. to 1.05 p.u. in the test network.

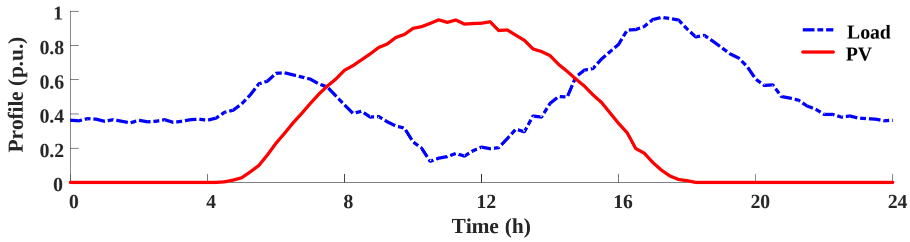

Fig. 2. The forecasting curves of DG and load.

Performance of mechanism parameter estimation. Using the historical operational data, it is estimated that the network parameters of the ADN are sufficient to establish a coordinated voltage control model. To account for measurement errors in the multi-source operational data, 0.1% standard deviation Gaussian distributed measurement noises are added to the true value. Fig. 3 presents accurate and estimated values for the components of the bus impedance matrix Z.

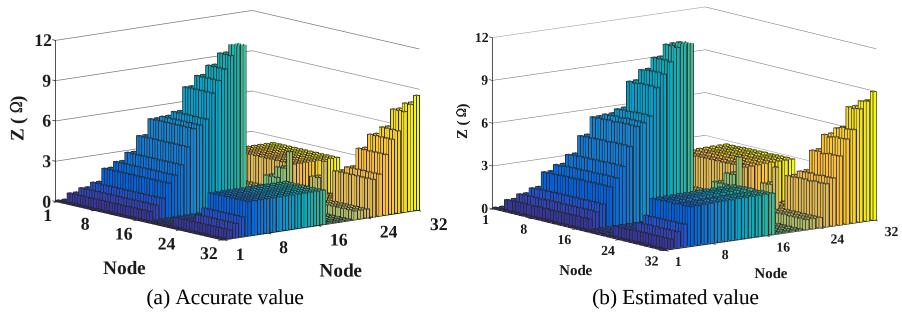

Fig. 3. The actual fluctuations of DG in different area.

Through inverting the bus impedance matrix Z, the parameters of line in ADN can be obtained. The estimation error of line parameters is shown in Fig. 4.

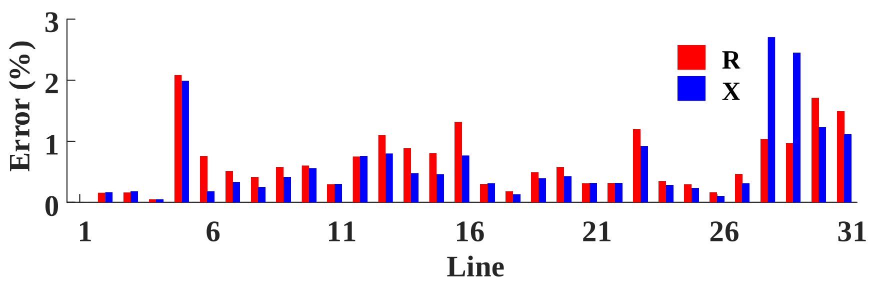

Fig. 4. The estimation error of line parameters.

It can be seen that the estimation error of the network parameters of ADN is less than 3%. This indicates accurate estimation of mechanistic parameters, supporting co-ordination of multiple devices.

Effectiveness analysis of data-driven based coordinative strategy. With the forecast data of loads and DGs, the strategy of multiple regulation devices are determined. Two scenarios are adopted to verify the effectiveness of the proposed data-driven based co-ordinated voltage control strategy.

Scenario I: There is no control strategy conducted on regulation devices, which can obtain the initial operational state of the ADN.

Scenario II: The control strategy of multiple regulation devices is determined with the estimated network parameters and forecast information.

The optimization results for the four scenarios are listed in Table I.

TABLE I

OPTIMIZATION RESULTS OF THE TWO SCENARIOS

Scenario	Minimum voltage (p.u.)	Maximum voltage (p.u.)	Voltage deviations (p.u.)	Power loss (kWh)
I	0.9219	1.0597	1942.4475	1180.8116
II	0.9484	1.0200	298.0456	1476.8004

In Scenario I, the significant uncertainties of the high penetration of DGs lead to the frequent voltage fluctuation and voltage deviation. The voltage profiles in Scenario I are shown in Fig. 5.

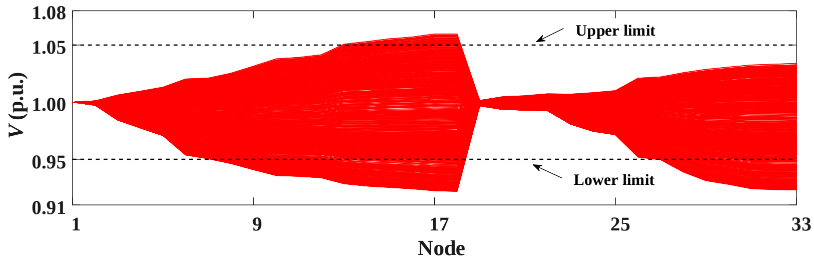

Fig. 5. The voltage profiles in Scenario I.

Based on the day-head forecast data and approximate physical parameters, the control strategy of multiple regulation devices can be obtained. The control strategies of discrete regulation devices in Scenario II are shown in Fig. 6.

Compared with the initial operation state in Scenario I, the voltage deviation of the distribution network is significantly alleviated. The voltage profiles in Scenario II are shown in Fig. 7.

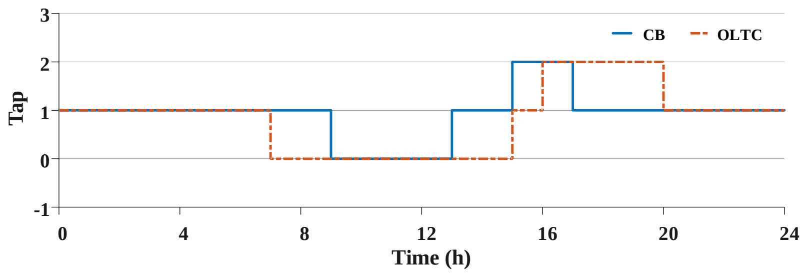

Fig. 6. The control strategies of discrete regulation devices.

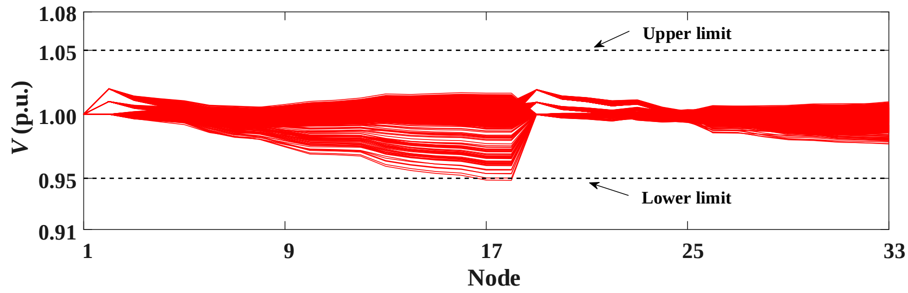

Fig. 7. The voltage profiles in Scenario II.

5 CONCLUSIONS

A data-driven voltage control strategy for ADN is proposed in this paper to effectively eliminate voltage violations. Firstly, data-driven methods are utilized to identify ADN's network parameters. Next, a coordinate voltage control model is established, which enables the cooperation of multiple regulation devices. By implementing this voltage control strategy, voltage violations can be significantly reduced, while simultaneously minimizing ADN's operating costs.

References

1. S. Su, G. Hu, X. Li, et al, "Analysis and power quality improvement in hybrid distributed generation system with utilization of unified power quality conditioner," Energy Eng., vol. 120, no. 10, pp. 2343-2368, 2023.
2. S. Liu, C. Zhou, H. Guo, et al, "Operational optimization of a building-level integrated energy system considering additional potential benefits of energy storage," Prot. Control Mod. Power Syst., vol. 6, 4, 2021.
3. H. Zhang, J. Chen, J. Yan, et al, "Urban power load profiles under ageing transition integrated with future EVs charging," Advances in Applied Energy, vol. 1, 100007, 2021.
4. G. Lei, C. Xu, "Optimal intelligent reconfiguration of distribution network in the presence of distributed generation and storage system," Energy Eng., vol. 119, no. 5, pp. 2005-2029, 2022.

5. X. Chen, M. B. Mcelroy, Q. Wu, et al, “Transition towards higher penetration of renewables: an overview of interlinked technical, environmental and socio-economic challenges,” J. Mod. Power Syst. Clean Energy, vol.7, no. 1, pp.1-8, 2019.
6. P. Yu, C. Wan, M. Sun, et al, “Distributed voltage control of active distribution networks with global sensitivity,” IEEE Trans. Power Syst., vol. 37, no. 6, pp. 4214-4228, 2022.
7. T. Niknam, “A new HBMO algorithm for multiobjective daily volt/var control in distribution systems considering distributed generators,” Appl. Energy, vol. 88, no. 3, pp. 778-788, 2011.
8. T. Tewari, A. Mohapatra, S. Anand, “Coordinated control of OLTC and energy storage for voltage regulation in distribution network with high PV penetration”, IEEE Trans. Sustain. Energy, vol. 12, no. 1, pp. 262-272, 2021.
9. N. Nazir, M. Almassalkhi, “Voltage positioning using co-optimization of controllable grid assets in radial networks”, IEEE Trans. Power Syst., vol. 36, no. 4, pp. 2761-2770, 2021.
10. F. Ding, Y. Zhang, J. Simpson, et al, “Optimal energy dispatch of distributed PVs for the next generation of distribution management systems,” IEEE Open Access Journal of Power and Energy, vol. 7, pp. 287-295, 2020.
11. G. C. Kryonidis, C. S. Demoulias, G. K. Papagiannis, “A two-stage solution to the bi-objective optimal voltage regulation problem,” IEEE Trans. Sustain. Energy, vol. 11, no. 2, pp. 928-937, 2020.
12. Z. Tang, D. J. Hill, T. Liu, et al, “Hierarchical voltage control of weak subtransmission networks with high penetration of wind power,” IEEE Trans. Power Syst., vol. 33, no. 1, pp. 187-197, 2018.
13. W. Jiao, J. Chen, Q. Wu, et al, “Distributed coordinated voltage control for distribution networks with DG and OLTC based on MPC and gradient projection,” IEEE Trans. Power Syst., vol. 37, no. 1, pp. 680-690, 2022.
14. X. Sun, J. Qiu, Y. Tao, et al, “Coordinated real-time voltage control in active distribution networks: an incentive-based fairness approach,” IEEE Trans. Smart Grid, vol. 13, no. 4, pp. 2650-2663. 2022.
15. N. Zhao, F. You, “New York State's 100% renewable electricity transition planning under uncertainty using a data-driven multistage adaptive robust optimization approach with machine-learning,” Adv. Appl. Energy, vol. 2, 100019, 2021.
16. D. Cao, W. Hu, J. Zhao, et al, “A multi-agent deep reinforcement learning based voltage regulation using coordinated PV inverters,” IEEE Trans. Power Syst., vol. 35, no. 5, pp. 4120-4123, 2020.
17. W. Wang, N. Yu, Y. Gao, et al, “Safe off-policy deep reinforcement learning algorithm for Volt-VAR control in power distribution systems,” IEEE Trans. Smart Grid, vol. 11, no. 4, pp. 3008-3018, 2020.
18. Z. Hou, S. Jin, “Data-driven model-free adaptive control for a class of MIMO nonlinear discrete-time system,” IEEE Trans. Neural Networks, vol. 22, no. 12, pp. 2173-2188, 2011.
19. S. Wang, J. Li, Z. Hou, et al, “Wind power compound model-free adaptive predictive control based on full wind speed,” CSEE J. Power Energy Syst., vol. 8, no. 6, pp. 1659-1669, 2022.
20. J. Chang, G. Lee, S. Oh, “Bus impedance matrix estimation using non-PMU measurements,” IEEE Trans. Power Syst., vol. 38, no. 2, pp. 1743-1746, 2023.